Supplemental Material: A Surface-Theoretic Approach for Statistical Shape Modeling

Felix Ambellan[0000−0001−9415−0859], Stefan Zachow[0000−0001−7964−3049], and Christoph von Tycowicz[0000−0002−1447−4069]

Therapy Planning Group, Zuse Institute Berlin, Berlin, Germany
{ambellan, zachow, vontycowicz}@zib.de

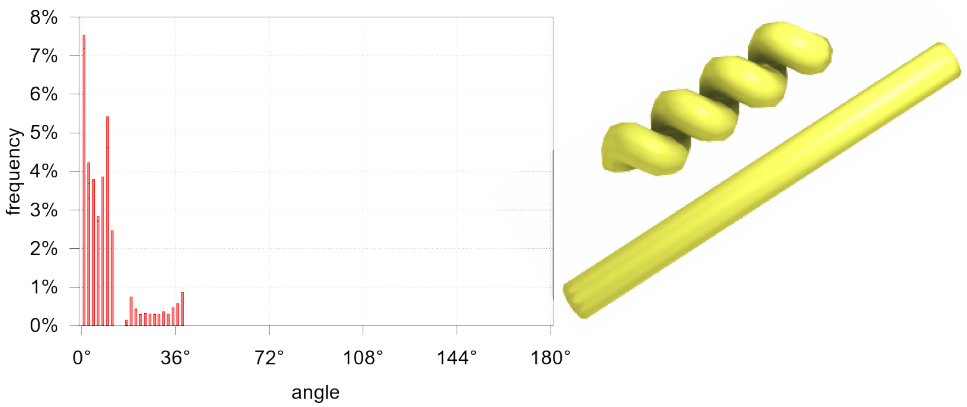

Fig. 1. (Supp. to Sec. 4 Validity) Histogram of angles between transition rotations (left) of the input shapes on the right. These relative transition rotations are all settled within the bijectivity region around the identity of the rotational logarithm, with angles in the interval $[3.2 \times 10^{-7}, 38.74]$ (degree).

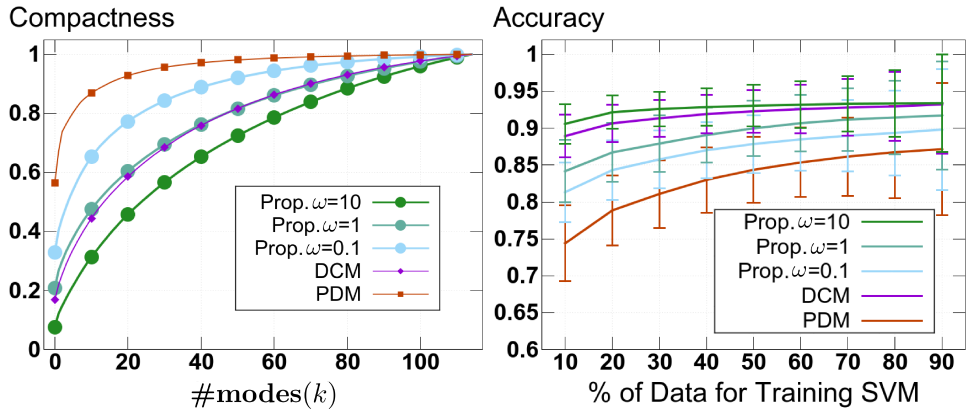

Fig. 2. (Supp. to Sec. 4 Compactness and Classification) Varying commensuration parameter ω indicates (i) inverse proportionality between ω and model compactness (left) and (ii) proportionality between ω and classification accuracy (right). In other words, the least compact model yields the highest classification accuracy.

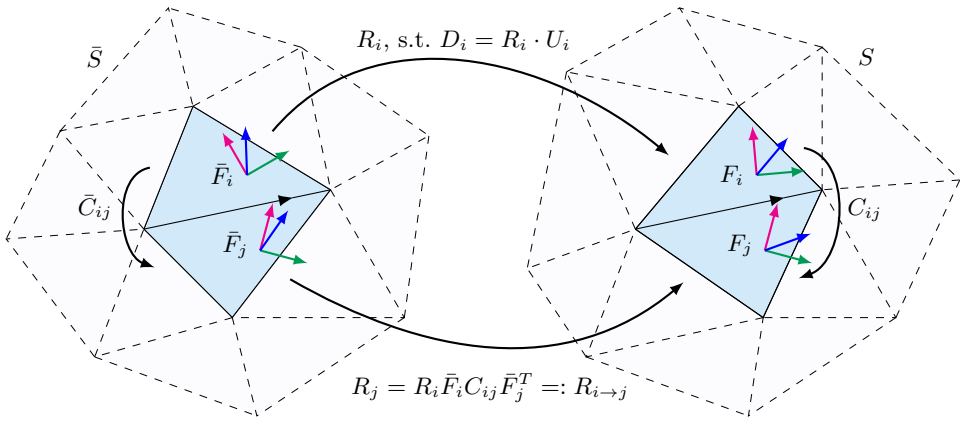

Fig. 3. (Supp. to Sec. 2 Discretization and Sec. 3) Relations between reference shape $\bar{S}$ (left) and shape $S = \phi(\bar{S})$, a deformation thereof (right), s.t. $D_i := \nabla\phi|_{\bar{T}_i}$. Note that each frame $F_i = R_i\bar{F}_i$ is defined solely on the respective triangle T_i and all neighboring frames are connected across the shared edge of their underlying triangles via $F_i C_{ij} = F_j$.

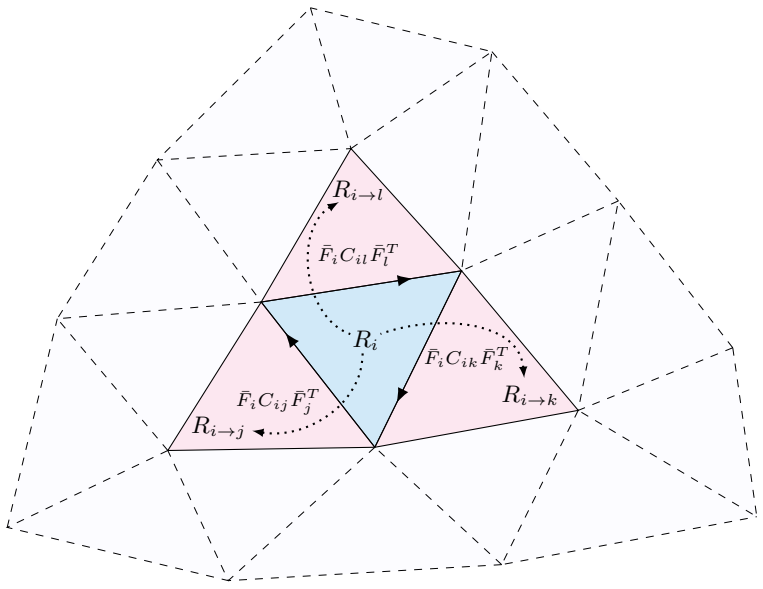

Fig. 4. (Supp. to Sec. 3) Neighboring relations employed in the local step of the integration procedure. Rotations R_i are connected by means of the transition rotations C_{ij}, s.t. we can formulate $R_i = \arg\min_{R\in\mathrm{SO}(3)} \sum_{s\in\mathcal{N}_i} \left\| D_s - R\bar{F}_i C_{is} \bar{F}_s^T U_s \right\|_2^2$. This problem can be solved in closed form utilizing polar decomposition (see Equation 1).

$$
\begin{aligned}
R_i &= \underset{R\in\mathrm{SO}(3)}{\arg\min} \sum_{s\in\mathcal{N}_i} \left\| D_s - R\bar{F}_i C_{is} \bar{F}_s^T U_s \right\|_2^2 \quad (\mathcal{N}_i \text{ - neighbors of triangle } i) \\
&\overset{\text{(A)}}{=\!=}_{\text{(B)}} \underset{R\in\mathrm{SO}(3)}{\arg\max} \sum_{s\in\mathcal{N}_i} \left\langle \tilde{D}_s, R \right\rangle_2 = \underset{R\in\mathrm{SO}(3)}{\arg\max} \left\langle \sum_{s\in\mathcal{N}_i} \tilde{D}_s, R \right\rangle_2 \\
&= \underset{R\in\mathrm{SO}(3)}{\arg\max} \left\langle \tilde{D}_{\mathcal{N}_i}, R \right\rangle_2 = \underset{R\in\mathrm{SO}(3)}{\arg\max} \left\langle \tilde{R}_{\mathcal{N}_i} \tilde{U}_{\mathcal{N}_i}, R \right\rangle_2 \quad \text{(polar decomposition)} \\
&= \tilde{R}_{\mathcal{N}_i}
\end{aligned}
$$

Where we take a glance at the two details (A) and (B):

$$
\left\| D_s - R\bar{F}_i C_{is} \bar{F}_s^T U_s \right\|_2^2 = \underbrace{\|D_s\|_2^2}_{\text{const.}} - 2 \left\langle D_s, R\bar{F}_i C_{is} \bar{F}_s^T U_s \right\rangle_2 + \underbrace{\left\| R\bar{F}_i C_{is} \bar{F}_s^T U_s \right\|_2^2}_{\text{const.}} \tag{A}
$$

$$
\begin{aligned}
\left\langle D_s, RF_i' C_{is} F_s'^{-1} U_s \right\rangle_2 &= \mathrm{tr}\left(D_s^T R F_i' C_{is} F_s'^{-1} U_s \right) = \mathrm{tr}\left(F_i' C_{is} F_s'^{-1} U_s D_s^T R \right) \\
&= \left\langle D_s U_s^T F_s' C_{is}^T F_i'^T, R \right\rangle_2 = \left\langle \tilde{D}_s, R \right\rangle_2
\end{aligned} \tag{B}
$$

Equation 1: (Supp. to Sec. 3) A calculation on how the transition rotations C_{is} determine the rotation R_i. This equation delivers the basis for the local step (D_s fix, solve for R_i) of the integration procedure and is a mathematical close up on Fig.4. Note that the problem reduces to the well-known orthogonal Procrustes problem.

Table 1. (Supp. to Sec. 4) List of (unique) patient ids from the OAI database used in the classification experiment. All cases can be found in the publicly available segmentations of the *OAI-ZIB* dataset (https://doi.org/10.12752/4.ATEZ.1.0) allowing for comparison with the shown experiment and reproduction thereof.

Healthy (KL 0/1)	Diseased (KL 4)
9008561 9258563 9510418	9246518 9391984 9631713
9013798 9304351 9517914	9256759 9393987 9638953
9017909 9331053 9582487	9263504 9413071 9642550
9036770 9333574 9601162	9266394 9414291 9660708
9036948 9341699 9617689	9267719 9421492 9672573
9039744 9341903 9645577	9271965 9422381 9680800
9089627 9355112 9655592	9284505 9430102 9689922
9108461 9383004 9718992	9287216 9439428 9691663
9116298 9391372 9750072	9301332 9457359 9695135
9120941 9394136 9854269	9326657 9467278 9700341
9132486 9397088 9876530	9331465 9469318 9710479
9141244 9397976 9878765	9340139 9470313 9745458
9153509 9433408 9879069	9349261 9475286 9750090
9171766 9440417 9907090	9364366 9477175 9760079
9184495 9460287 9916140	9365968 9477358 9781749
9189553 9474901 9967815	9375317 9508335 9858216
9207016 9486748 9973322	9379276 9517311 9895555
9211049 9488834 9978579	9389580 9557454 9933836
9245519 9501871 9988421	9391061 9568504 9943227
9504627	9604541